

掺杂铜的介孔 SiO₂ 微球的制备以及对亚甲基蓝的吸附

曹 渊* 邹函君 魏红娟 文 毅 王亚涛

(重庆大学化学化工学院, 重庆 400044)

摘要: 通过水热法在室温下合成了不同铜含量的介孔 SiO₂ 微球(Cu-MSM)。目的在于研究吸附剂量、MB 的初始浓度以及吸附时间对 Cu-MSM 从溶液中移除亚甲基蓝(MB)吸附性能的影响。结果表明, 当增加 Cu-MSM 的量时, MB 的去除率会大大提高; 掺杂铜的介孔 SiO₂ 微球可以通过吸附去除水溶液中的亚甲基蓝。最后, 简要探讨了亚甲基蓝的吸附机理。

关键词: 亚甲基蓝; Cu-MSM; 吸附

中图分类号: O614.121; TQ424.26

文献标识码: A

文章编号: 1001-4861(2012)08-1705-07

Preparation and Methylene Blue Adsorption of Mesoporous Silica Microspheres Doped with Copper

CAO Yuan* ZOU Han-Jun WEI Hong-Juan WEN Yi WANG Ya-Tao

(College of Chemistry & Chemical Engineering, Chongqing University, Chongqing 400044, China)

Abstract: Mesoporous silica microspheres doped with various amounts of copper (Cu-MSM) were synthesized using a hydrothermal method at room temperature. The aim of the present work is to explore the effect of adsorbent dosage, initial concentration of methylene blue (MB), and contact time on the adsorption performance of Cu-MSM for the removal of MB from aqueous solutions. The results show that the dye removal can be greatly improved by increasing the Cu-MSM dosage. The results also indicate that Cu-MSM can be used for the removal of MB from aqueous solutions by adsorption. Finally, the adsorption mechanism of MB is discussed.

Key words: methylene blue; Cu-MSM; adsorption

0 Introduction

In recent years, dyestuff effluents as highly colored wastewater have attracted more and more concerns. The runoffs (colored wastewaters) from manufacturing and textile industries were discarded into rivers and lakes, altering the biological stability of surrounding ecosystems^[1]. MB is the most commonly used dyestuff for dyeing cotton, wood and silk. On inhalation, it can give rise to short periods of rapid or difficult breathing

while ingestion through the mouth produce a burning sensation and may cause nausea, vomiting, profuse sweating, mental confusion and methemoglobinemia^[2-4].

The degradation of some kinds of dye molecules is rather difficult because they are very stable against light and oxidation reactions. Various physical, chemical, and biological treatments have recently been applied for dye wastewater treatment, such as electrocoagulation, chemical oxidation, biodegradation^[5], and adsorption. Adsorption is the most commonly used method for dye

收稿日期: 2011-11-22。收修改稿日期: 2012-04-24。

中央高校基础研究基金(No.CDJXS10221136)、科技部国际技术计划合作项目(No.1010104520100174)、“211 工程”第三阶段训练和中央高校基础研究基金(CDJXS10220007)资助项目。

*通讯联系人。E-mail: caoyuan@cqu.edu.cn.

removal, the mechanism of which is assumed to be an ion exchange process^[6]. The adsorption characteristics of MB dyes on various adsorbents, such as activated carbon, agricultural waste, silica, clay, industrial solid wastes, sewage sludge^[7] have been extensively investigated. Adsorption on commercial activated carbon is an effective but expensive process for the removal of dyes from dye wastewater, and the regeneration of spent activated carbon is relatively difficult^[8]. Therefore, the development of low-cost and effective methods for the wastewater treatment is necessary.

Recent years bring new developments in syntheses of new materials characterized by well-dened porous structure in the range of mesopores^[9-12]. It has aroused considerable attention on the application of ordered mesoporous material with large surface area and pore volume on waste water treatment. Therefore, in many applications good reproducibility of adsorbent syntheses and high uniformity of their porous structure are the keys to success^[13]. The pore channels of mesoporous SiO₂ are ordered and adjustable, especially, mesoporous SiO₂ contains many silicon groups spread over the matrix. The silicon groups tend to react with polar compounds^[14]. Besides, alkaline medium is considered to be favorabl to adsorption^[15].

In this study, mesoporous silica microspheres doped with copper (Cu-MSM) are used as adsorbents to remove MB dye from aqueous solutions via chemical activation. The effects of various parameters, such as contact time, adsorbent dosage, and initial dye concentration, on MB adsorption were investigated. The chemical activation process lowers energy costs and shortens the treatment duration.

1 Experimental

1.1 Preparation and characterization of Cu-MSM adsorbent

Three MSM samples doped with copper were synthesized using a hydrothermal method. Approximately 3.0 g of cetyl trimethylammonium bromide was dissolved in 360 mL of ethanol and 270 mL of distilled water and stirred until clear at room

temperature. Thereafter, x g of CuSO₄ (where $x=0.05$, 0.1, and 0.2) and 4.2 mL of ammonia were added to the mixture. The resulting solution was stirred for 0.5 h and then 17.4 mL of tetraethyl orthosilicate was added. This mixed solution was stirred for only 0.5 min and allowed to stand for 12 h at ambient temperature. The sample was filtered, washed with distilled water, and then dried. The dried materials were calcined at 550 °C for 6 h to decompose the surfactant. Finally, the gray powders, as mesoporous silica microspheres doped with copper, were designated Cu-MSM-1, Cu-MSM-2, and Cu-MSM-3, representing MSM samples with 0.05, 0.1, and 0.2 g of CuSO₄, respectively. The prepared Cu-MSM samples were stored in an airtight container for the adsorption experiments.

Powder X-ray diffraction (XRD) data were recorded on a diffractometer (Shimadzu XRD-6000) with Cu K α radiation ($\lambda=0.154$ 18 nm) at 40 kV and 35 mA, scan rate 0.02° (2θ)·s⁻¹ within a range of 20°~80° (2θ). Fourier transform infrared (FTIR) spectra were performed in KBr discs using an FTIR spectrophotometer (Shimadzu IR Affinity-1,) in the range of 4 000~400 cm⁻¹. A FEI SIRION100S canning electron microscopy (SEM) was carried out at operating voltages varying from 1.0 kV to 30.0 kV. Nitrogen sorption isotherms were measured at -196.61 °C in relative pressure range of 0~1.0 using micromeritics on ASAP 2020 V 3.01 H volumetric adsorption analyzer.

1.2 Experimental method

Adsorption experiments were undertaken in a batch reactor with 250 mL capacity by mixing 4.5~85 mg of Cu-MSM with 20 mL dye solutions (15~105 mg·L⁻¹) at room temperature. The beakers were then stirred with different adsorption times in visible light. The samples were then centrifuged for 10 min at 4 000 r·min⁻¹ and the residue concentration in the supernatant solution was analyzed using a UV-Vis spectrophotometer by monitoring the absorbance changes at a wavelength of maximum absorbance (665 nm). Dye removal was calculated as follows:

$$\text{dye removal (\%)}=(1-A_t/A_0)\times 100\%$$

where A_t and A_0 are absorbance of MB in solution at time $t=t$ and $t=0$, respectively.

1.2.1 Effect of adsorbent dosage

The sample was added to each 20 mL volume of 45 mg·L⁻¹ MB solution. The amount of Cu-MSM was 4.5, 10, 20, 40 and 85 mg and the experiments were carried out at room temperature for 30 min.

1.2.2 Effect of initial dye concentration

10 mg sample of Cu-MSM was added to each 20 mL MB solution. The initial concentrations of dye solution tested were 15, 45, 75 and 105 mg·L⁻¹ and the experiments were carried out at room temperature for 30 min.

1.2.3 Effect of contact time

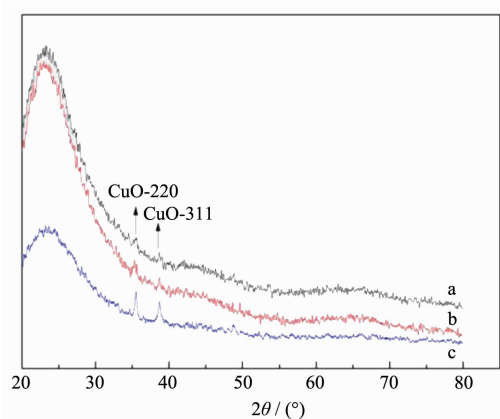
10 mg sample of Cu-MSM was added to each 20 mL MB solution. The initial concentrations of dye solution tested were 15, 45 and 105 mg·L⁻¹ and the experiments were carried out at room temperature for 2, 5, 15, 30 and 60 min.

2 Results and discussion

2.1 Characterization of adsorbents

2.1.1 X-ray diffraction (XRD) analysis

Fig.1 shows wide-angle (2°~80°) XRD patterns of Cu-MSM. A wide diffraction peak at 2θ of 20°~35° were clearly observed in XRD patterns of a, b, c. The patterns indicate the hexagonal lattice of the mesoporous sample^[16-17] and three samples of Cu-MSM still keep the uniform pore structure. The two strongest characteristic diffraction peaks of CuO are observed at 2θ of 35.5° and 38.7°, demonstrating that CuO has been incorporated into the framework and/or walls of the



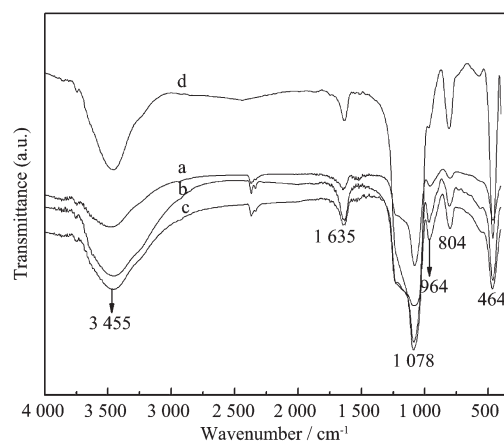
(a) Cu-MSM-1; (b) Cu-MSM-2; (c) Cu-MSM-3

Fig.1 XRD patterns of three samples

silica matrix. The peak intensity of the samples weakens as the Cu loading increases.

2.1.2 FTIR spectra analysis

The FTIR results are shown in Fig.2. The spectra display a number of absorption peaks, indicating the complex nature of the material examined. The characteristic absorption peaks of the sample (a, b, c, d) are observed, respectively, at 804 and 464 cm⁻¹ (bending vibrations of Si-O-Si), 1 087 cm⁻¹ (asymmetric stretching vibrations of Si-O-Si), 1 635 cm⁻¹ (deformational vibrations of absorbed water molecule) and 3 455 cm⁻¹ (-OH bond stretching of the surface silanols groups)^[18-20]. In addition, the band at 964 cm⁻¹ probably arises from both Si-O-H and Si-O-Cu stretching vibrations. This proves the successful synthesis of Cu-MSM.



a: Cu-MSM-1; b: Cu-MSM-2; c: Cu-MSM-3; d:MSM

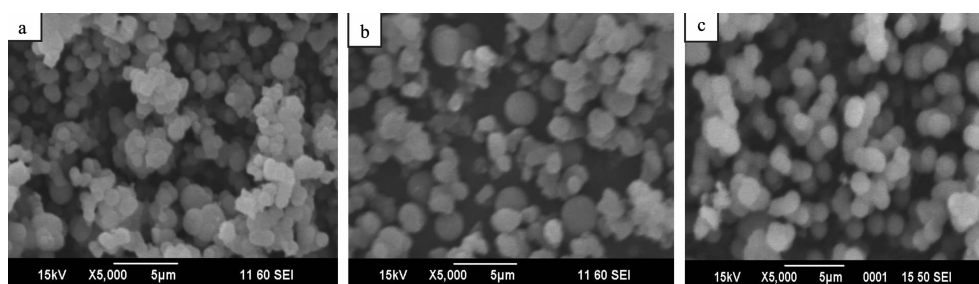
Fig.2 FTIR spectra of the sample

2.1.3 SEM analysis

Scanning electron micrographs of calcined samples are shown in Fig.3. It has been found that the materials show a homogeneous spherical shape distribution. The particles for sample show agglomeration seriously, but the SEM image for particles b are unified rod-shape like sample c.

2.1.4 N₂ adsorption-desorption analysis

The N₂ adsorption-desorption isotherms of Cu-MSM are shown in Fig.4. It shows that all samples display a type IV isotherm with H1 hysteresis and a sharp increase in volume adsorbed at $P/P_0 = 0.2 \sim 0.4$, characteristic of highly ordered mesoporous materials^[21]. This is identified as a slow rate of increase in N₂ uptake



(a) Cu-MSM-1; (b) Cu-MSM-2; (c) Cu-MSM-3

Fig.3 SEM photograph of a, b, c

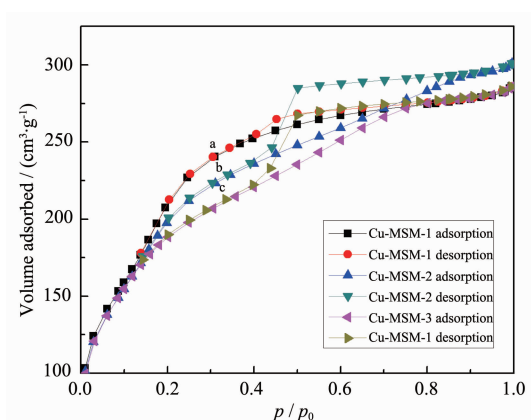


Fig.4 Nitrogen adsorption isotherms of a, b, c; (a) Cu-MSM-1, (b) Cu-MSM-2, (c) Cu-MSM-3;
 p -Pressure of the adsorbate; p_0 -Saturated vapor pressure of liquid adsorbate at adsorption temperature=77 K

at a low relative pressure, corresponding to monolayer multilayer adsorption on the pore walls. The key feature is that there are small hysteresis loops attributed to capillary condensation of nitrogen within mesoporous channels. The data of the average pore size, BET surface area and pore volume of Cu-MSM are summarized in Table 1. The results suggest that the material is with very low surface area and total pore volume.

2.2 Adsorption of methylene blue

2.2.1 Effect of adsorbent dosage

The adsorption of MB was examined by changing the adsorbent content (4.5 mg to 85 mg) in the test

solution at room temperature for a contact time of 30 min and at an initial dye concentration of $45 \text{ mg} \cdot \text{L}^{-1}$. The dye removal percentages at different doses of the three adsorbents are presented in Fig.5. MB removal increases with increasing adsorbent mass only for Cu-MSM contents between 4.5 and 20 mg, whereas slight changes are observed from 40 mg to 85 mg. Cu-MSM has a large BET surface area, a typical mesoporous material characteristics; thus, it has high adsorption capacity. The number of active adsorption sites increases with the increase in surface area resulting from the increase in adsorbent dosage. For example, as the Cu-MSM-1 powder is increased from 4.5 mg to 85 mg, the percentage of adsorbed MB increases from 51% to 95%. The increase in dye removal rate is caused by the increase in adsorbent surface area and availability of more adsorption sites^[22]. However, a higher dosage cannot drastically improve the dye removal rate. The MB removal rate reaches 97% when 20 mg of Cu-MSM-3 is added to the solution and 98% when 85 mg of Cu-MSM-3 is added. Mesoporous silica microspheres doped with copper are also observed to increase MB adsorption; the greater the Cu content, the higher the dye removal rate (Fig.5). Approximately 41%, 85%, 91%, and 93% of the MB could be adsorbed by 10 mg of Cu-MSM, Cu-MSM-1, Cu-MSM-2, and Cu-MSM-3, respectively. Adsorption of organics is believed to depend on the pore structures and surface chemical

Table 1 Characteristics of the adsorbent

	d_{100} / nm	a_0 / nm	Average pore size / nm	Wall Thickness / nm	BET Surface Area / ($\text{m}^2 \cdot \text{g}^{-1}$)	Pore Volume / ($\text{cm}^3 \cdot \text{g}^{-1}$)
Cu-MSM-1	2.9	3.4	2.2	1.2	802	0.44
Cu-MSM-2	3.0	3.4	2.4	1.0	754	0.46
Cu-MSM-3	3.5	4.0	2.5	1.5	701	0.44

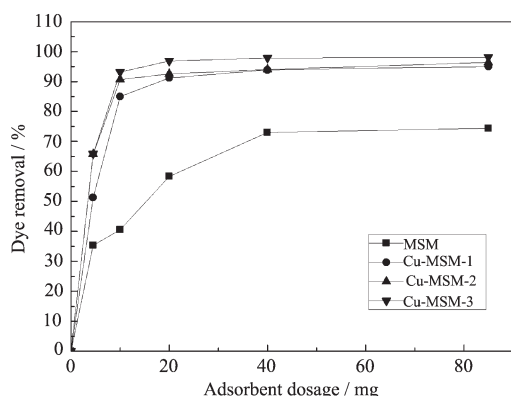


Fig.5 Effect of different adsorbent dosages on MB removal at room temperature, contact time of 30min and MB initial concentration of $45 \text{ mg} \cdot \text{L}^{-1}$

properties of mesoporous silica microspheres. Therefore, MB adsorption depends largely on the chemistry of the adsorbent surface and Cu contents.

2.2.2 Effect of MB initial concentration

Fig.6 shows the removal of different initial concentrations of MB by 10 mg of Cu-MSM for 30 min. At low MB concentrations, a higher adsorption efficiency is observed. When 10 mg of Cu-MSM-3 is added to MB solution from $15 \text{ mg} \cdot \text{L}^{-1}$ to $105 \text{ mg} \cdot \text{L}^{-1}$, the dye removal rate decreases from 94% to 90%. Mesoporous silica microspheres doped with copper also increase MB adsorption. Cu-MSM-3 has a greater adsorption efficiency compared with Cu-MSM-2 and Cu-MSM-1 at the same MB concentration. When $45 \text{ mg} \cdot \text{L}^{-1}$ of the dye is mixed with Cu-MSM-3, Cu-MSM-2, and Cu-MSM-1, removal rates of 93%, 90%, and 85%, respectively, are obtained.

2.2.3 Effect of contact time

MB adsorption experiments were conducted using

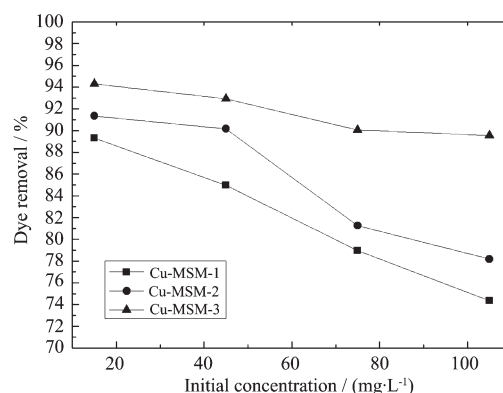
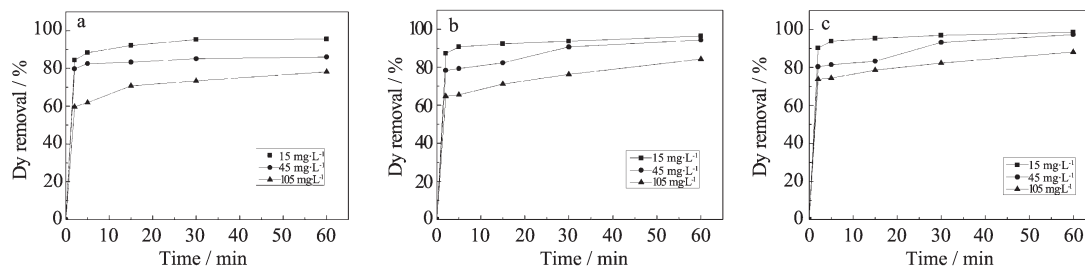


Fig.6 Effect of different initial concentrations on MB removal at room temperature, contact time of 30 min and adsorbent dosage of 10 mg

Cu-MSM-1, Cu-MSM-2, and Cu-MSM-3 at a constant adsorbent dosage (10 mg) and room temperature with different MB concentrations by varying the contact time (2, 5, 15, 30, and 60 min). Plots of the adsorption capacity versus contact time at various initial MB concentrations are shown in Figs.7a to 7c. The adsorption percentage of the dye increases with increasing contact time. The removal of MB by adsorption on adsorbents is rapid during the initial stages of treatment and then becomes slow and stagnant with increasing contact time. The contact time curve shows that the dye removal rate is rapid within the first 5 min of exposure because of surface adsorption, and the three adsorbents exceed 90% removal within 10 min. The equilibrium time between the adsorbents and MB solution is about 30 min. All subsequent adsorption experiments were performed for 60 min, a period assumed to be largely ample for performing all experiments. During initial dye adsorption, dye molecules rapidly reach the boundary layer by mass



(a) Cu-MSM-1; (b) Cu-MSM-2; (c) Cu-MSM-3

Fig.7 Effect of contact time on MB removal at room temperature, adsorbent dosage of 10 mg

transfer and then slowly diffuse from the boundary layer lm onto the adsorbent surface because many of the available external sites are occupied. Finally, the molecules diffuse into the porous structure of the adsorbent^[23]. Fig.7a shows that the equilibrium dye removal rate decreases from 95% to 73% with increasing initial MB concentration from $15 \text{ mg} \cdot \text{L}^{-1}$ to $105 \text{ mg} \cdot \text{L}^{-1}$. The lower the initial concentration of MB, the higher the dye removal rate. The same phenomenon is also presented in Fig.7b and Fig.7c.

2.3 Adsorption mechanism analysis

Amorphous silica has gained considerable attention because of the chemical reactivity of their hydrophilic surface due to the presence of silanol groups. Their porous texture, high surface area, and mechanical stability also make them attractive candidates as adsorbents for decontamination applications^[24]. However, MB has difficulty in not only accessing the pure mesoporous silica microsphere from the surface but also accumulating in large amounts on the internal structure of the adsorbents because of the longer channels and smaller diameters of the mesopores, as well as their parallel direction to the substrate^[25]. Incorporation of aluminum into the structure of MCM-41 materials via isomorphous substitution of aluminum for silicon has been reported to generate ion exchange sites in these mesoporous molecular sieves^[26-28]. Therefore, MB adsorption on Cu-MSM is also likely to be dominated by ion exchange processes. Better dispersion is achieved by converting MSM to Cu-MSM and generating ion exchange sites. After incorporation of Cu into mesoporous silica, cationic MB generates exchanges with Cu^{2+} and is adsorbed onto MSM resulting in Si-O-MB. Meanwhile, Cu^{2+} and Cl^{-} of MB produce $[\text{CuCl}_4]^{2-}$. In this study, Cu-MSM displays strong UV absorption capability in visible light, leading to a decrease in the absorbance of MB with increasing Cu content. This observation suggests a decrease in MB concentration. The maximum MB removal rate obtained by Cu-MSM-1, Cu-MSM-2, and Cu-MSM-3 for 60 min are 95%, 96%, and 98%, respectively. Interestingly, the surface area of Cu-MSM decreases with increasing Cu content. However, both

the unit cell dimension and d_{100} increase with increasing Cu content, suggesting dispersion of MB into MSM and more complete displacement of Cu^{2+} .

3 Conclusions

The adsorption of MB from aqueous solutions using Cu-MSM powder was investigated, and various impact factors, such as adsorbent dosage, initial MB concentration, and contact time, were optimized. In adsorption experiments, the results show that Cu-MSM exhibits a much higher dye removal rate than MSM. The adsorption copper content has a certain influence on the removal rate, such that the greater the Cu content, the higher the dye removal rate. In view of such results, the extent of adsorption of MB onto Cu-MSM increases with the amount of Cu-MSM and decreases with the initial concentration of the dye solution. The removal rate of $45 \text{ mg} \cdot \text{L}^{-1}$ MB by 85 mg of Cu-MSM-1, Cu-MSM-2, and Cu-MSM-3 is 95%, 96%, and 98%, respectively, after 30 min. Adsorption experiments indicate that Cu-MSM is an efficient adsorbent for the removal of MB from aqueous solutions. Significant MB adsorption also shows that Cu-MSM is suitable for the treatment of colored effluent waters.

References:

- [1] Sheng J, Xie Y, Zhou Y. *Appl. Clay Sci.*, **2009**,**46**:422-424
- [2] Ghosh D, Bhattacharyya K G. *Appl. Clay Sci.*, **2002**,**20**(6): 295-300
- [3] Tan I A W, Ahmad A L, Hameed B H. *J. Hazard. Mater.*, **2008**,**154**(1/2/3):337-346
- [4] Tan I A W, Ahmad A L, Hameed B H. *Desalination*, **2008**,**225**(1/2/3):13-28
- [5] El-Sheekh M M, Gharieb M M, Abou-El-Souod G W. *Int. Biodeter. Biodegr.*, **2009**,**63**:699-704
- [6] Wang C C, Juang L C, Hsu T C, et al. *J. Colloid Interface Sci.*, **2004**,**273**: 80-86
- [7] Rafatullah M, Sulaiman O, Hashim R, et al. *J. Hazard. Mater.*, **2010**,**177**: 70-80
- [8] Song J Y, Zou W H, Bian Y Y, et al. *Desalination*, **2011**, **265**:119-125
- [9] Kresge C T, Leonowicz M E, Roth W J, et al. *Nature*, **1992**, **359**:710-712

- [10]Zhao D, Huo Q, Feng J, et al. *J. Hazard. Mater.*, **1998**,**120**: 6024-6036
- [11]Joo S H, Jun S, Ryoo R. *Microporous Mesoporous Mater.*, **2001**,**44-45**:153-158
- [12]Kim J, Lee J, Hyeon T. *Carbon*, **2004**,**42**(12/13):2711-2719
- [13]Marczewski A W. *Appl. Surf. Sci.*, **2010**,**256**:5145-5152
- [14]Al-Ghouti M A, Khraishen M A M, Allen S J, et al. *J. Environ. Manage.*, **2003**,**69**(3): 229-238
- [15]Ma Y L, Xu Z R, Guo T, et al. *J. Colloid Interf. Sci.*, **2004**, **280**:283-288
- [16]Yu K, Gu Z C, Ji R N, et al. *J. Catal.*, **2007**,**252**:312-320
- [17]Charnay C, Begu S, Tourne-Peteilh C, et al. *Eur. J. Pharm. Biopharm.*, **2004**,**57**:533-540
- [18]Choi J S, Kim D J, Chang S H, et al. *Appl. Catal. A*, **2003**, **254**(2):225-237
- [19]Perez-Quintanila D, Del Hierro I, Fajardo M, et al. *Microporous Mesoporous Mater.*, **2006**,**89**:58-68
- [20]Lesaint C, Lebean B, Marichal C. *Microporous Mesoporous Mater.*, **2005**,**83**: 76-84
- [21]Das D, Lee J F, Cheng S. *J. Catal.*, **2004**,**223**:152-160
- [22]Mall I D, Srivastava V C, Agarwal N K. *Dyes Pigm.*, **2006**, **69**(3):210-223
- [23]Senthilkumaar S, Varadarajan P R, Porkodi K, et al. *J. Colloid Interface Sci.*, **2005**,**284**:78-82
- [24]Rafatullaha M, Sulaimana O, Hashima R, et al. *J. Hazard. Mater.*, **2010**,**177**:70-80
- [25]Du J, Lai X Y, Yang N L, et al. *J. Am. Chem. Soc.*, **2011**,**5**: 590-596
- [26]Wei D, Wang H, Feng X B, et al. *J. Phys. Chem. B*, **1999**, **103**(12):2113-2121
- [27]Bohlmann W, Michel D. *Stud. Surf. Sci. Catal.*, **2001**,**202**: 421-426
- [28]Zanjanchi M A, Asgari S. *Solid State Ionics*, **2004**,**171**(3/4): 277-282